Molecular Association and Reactivity of the Pyridine Dimer Cation

Amol Tagad and G. Naresh Patwari*

Department of Chemistry, Indian Institute of Technology Bombay, Powai, Mumbai 400076 INDIA

Email: naresh@chem.iitb.ac.in

Dedicated to the memory of Professor Takayuki Ebata

ABSTRACT

A recent experimental report has identified the formation of C–N hemi-bonded pyridine dimer cation following vacuum ultraviolet near-threshold photoionization [*J. Phys. Chem. Lett.* **2021**, *12*, 4936–4943]. Herein, the dynamics and consequent reactivity of the pyridine dimer cation was investigated employing Born-Oppenheimer Molecular Dynamics (BOMD) simulations. The neutral anti-parallel π-stacked pyridine dimer is transformed to a non-covalently interacting C–H···N hydrogen-bonded structure which can lead to proton transfer. Additionally, C–N and N–N bonded adducts were formed in the cationic state. Further, metastable C–H···H–C bonded cationic was observed, which rearranges to N–N bonded adduct. In contrast to the experimental observation, migration of the proton to the α position was not observed in the C–N bonded adduct owing to a high barrier of about 2 eV. The observed trends in the molecular association, proton transfer and formation of pyridinium cations are a consequence of roaming dynamics of one pyridine moiety over the other in the cationic state.

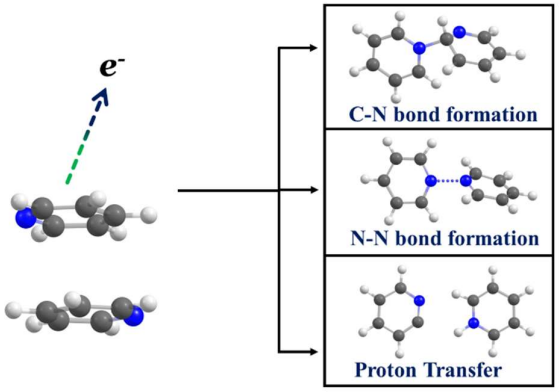

INTRODUCTION

Various non-covalent interactions involving aromatic compounds are pivotal in shaping the structure and properties of molecular clusters. Among these interactions, the benzene dimer and other substituted aromatic molecules serve as fundamental models for π-π stacking interaction, even though the π-stacked benzene dimer structure has not been observed experimentally.[1–3] On the other hand nitrogen containing heterocyclic compounds like pyridine and pyrimidine also demonstrate π-π stacking and n-π interactions.[4–7] Electronic structure calculations reveal that pyridine dimer exhibits several possible configurations, including π-stacked displaced antiparallel, T-shaped, and hydrogen-bonded structures, even though only a π-stacked displaced antiparallel and hydrogen-bonded structures were observed in the gas phase,[6] and in Ne matrices at 4K.[8] The ^{14}N NMR spectra and computational studies revealed that the ordered structure of non-flat pyridine dimer, held together by weak hydrogen bonding interaction.[9] On the other hand, the cation-π interactions of pyridine play a pivotal role in shaping protein structures, promoting self-association, influencing molecular crystallization,[10] and facilitating molecular recognition processes.[11–13] In the gas phase, pyridine radical cation and protonated pyridine were investigated using mass spectrometry, collision-induced dissociation,[14] ion mobility,[15] ion trap,[16] low-temperature Fourier transform spectroscopy.[17]

The proton affinities of various mono and bi-radicals within the pyridine system were determined using a linear quadrupole ion trap (LQIT) and a Fourier-transform ion cyclotron resonance mass spectrometer (FT-ICR).[18] These investigations unveiled that pyridine possesses the highest proton affinity, whereas bi-radicals of pyridine exhibit a lowering of the proton affinity due to their electron deficiency. Additionally, the proton affinity was found to be influenced by the specific location of the radical site. Radicals situated away from the nitrogen (N) atom in the pyridine ring displayed the highest proton affinity among the studied configurations.[18] In recent work, Feng *et al.* reported the formation of a hemi-bonded covalent C–N bond accompanied by proton migration in pyridine dimer cation following near-threshold vacuum ultraviolet photoionization of pyridine dimer, which is formed via a α-distonic (charge center and separate radical site) intermediate.[7] Interestingly, it was observed that the presence of an unpaired electron at another site of the ion does not significantly impact hydrogen bonding interactions.[19] This work aims to investigate and understand the dynamics and reactivity of pyridine dimer in the cationic state using Born-Oppenheimer molecular dynamics (BOMD) simulations.

METHODOLOGY

The dynamics of the pyridine dimer cation leading to either fragmentation or otherwise, were investigated using Born-Oppenheimer molecular dynamics (BOMD) simulations. The pyridine dimer in the ground state is a displaced anti-parallel π-stacked structure, as revealed by infrared-vacuum ultraviolet (IR-VUV) experiments,[6] shown in Figure 1. The coordinates of the input structure were obtained from Ref. 6 wherein the centre-of-mass to centre-of-mass (COM–COM) distance between the two pyridine rings is 3.47 Å. To begin with, the pyridine dimer cation was kept at the centre of a cubic box (25 Å) with periodic boundary conditions, and the system was equilibrated in an NVT ensemble using a Nose-Hoover thermostat[20] at 30K for a simulation time of 1.4 ps. Several snapshots from the NVT equilibration process were randomly chosen and unrestrained BOMD simulations were carried out in an NVE ensemble. The BOMD simulations were carried out using the QUICKSTEP module implemented in CP2K software,[21,22] with Becke-Lee-Yang-Parr (BLYP) functional in combination with double ζ valence potential (DZVP) basis set and auxiliary plane wave were used to expand the valence shell electron density along with Goedecker-Teter-Hutter (GTH) pseudopotentials for the core electrons.[23,24] The electron density was represented using the hybrid Gaussian and plane wave (GPW) method with a cut-off of 400 Ry. Each simulation trajectory was for a maximum duration of up to 10 ps, with an integration time step of 1.0 fs. The NVE simulations were performed over a temperature range from 70 to 200 K. A total of 133 trajectories were simulated and the distance between the centre-of-masses of the two pyridine moieties was evaluated along the trajectory. More than half of the trajectories simulated at temperatures of 150 K and above result in fragmentation with the distance between the centre-of-masses greater than 0.7 nm over the course of the trajectory. The number of unfragmented trajectories was 79, which were analyzed by examining the interatomic distances between the two pyridine moieties in the final snapshot of the trajectory,

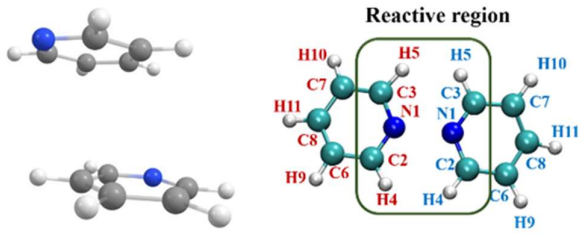

Figure 1. The π-stack displaced antiparallel initial structure of the pyridine dimer used as the starting structure(left). Labeling of atoms within the reactive region of pyridine dimer cation (right).

using the binary matrix method.[25] Further, the structures obtained at the end of 10 ps trajectory were optimized at BLYP/6-311++G(d,p) and ωb97XD/aug-cc-pVDZ levels of theory using the Gaussian-09 suite of programs.[26]

RESULTS AND DISCUSSION

The dynamical nature of the pyridine dimer cation was accessed by evaluating the COM–COM distances between the two pyridine moieties along the trajectory, shown in Figure 2. In all the reactive trajectories, the roaming of one pyridine ring over the other was observed with the COM–CO distance in the range of 0.35 to 0.7 nm.[27] Since a wide variety of reactive pyridine dimer cations have been reported,[7] the structure classification was carried out using the binary matrix method.[25] In this method, interatomic distances in the contact matrix were converted into binary logic (1 or 0) with the smallest distance being 1 and all the other elements as 0. Even though the interatomic contact matrix is 11x11 dimensional, in the case of pyridine dimer cation, a reduced dimensional 5x5 matrices were adequate to analyze the reactivity pattern to a larger extent (73 out of 79) as shown in Figure 1, while the remaining 6 trajectories showed reactivity outside the reduced dimensional 5x5 matrix (Figure S1, see the Supporting Information). Based on the binary matrix method, four prominent structural patterns

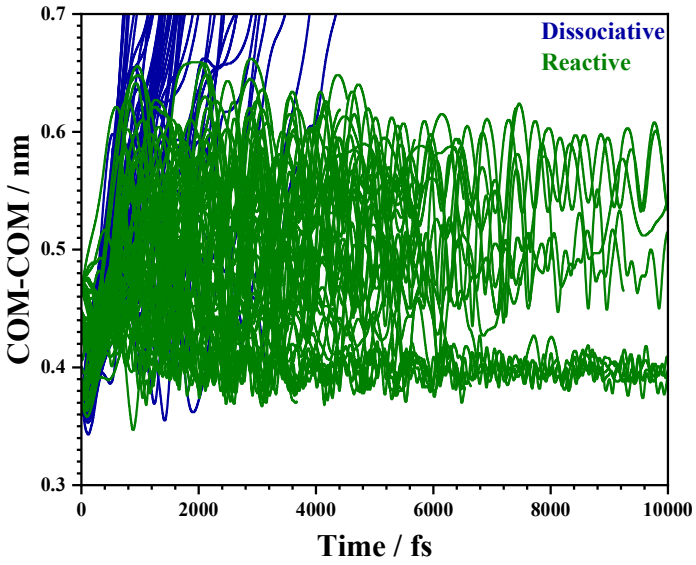

Figure 2. COM–COM distance between the two pyridine rings plotted as a function of simulation time. A total of 129 trajectories were simulated in the temperature range of 70-200 K of which 52 were dissociative (blue) and 77 were reactive (green).

were observed (see Figure S2), which include **[CH···N]** hydrogen bonded dimer (42+5 trajectories;61%), **[C–N]** bonded adduct (13+1 trajectories; 18%), **[N–N]** bonded adduct (10 trajectories; 13%) and CH···H–C bonded dimer (6 trajectories; 8%). Further, two of the **[CH···N]** trajectories result in proton transfer to yield **[PyH–Py]** structure. However, the formation of the associative/reactive dimer cations did not show any temperature dependence (Table S1, see the SI).

The molecular association and the reactivity of pyridine dimer cation starting from the initial π-stacked conformation is modulated by the roaming mechanism,[27] wherein one pyridine moiety

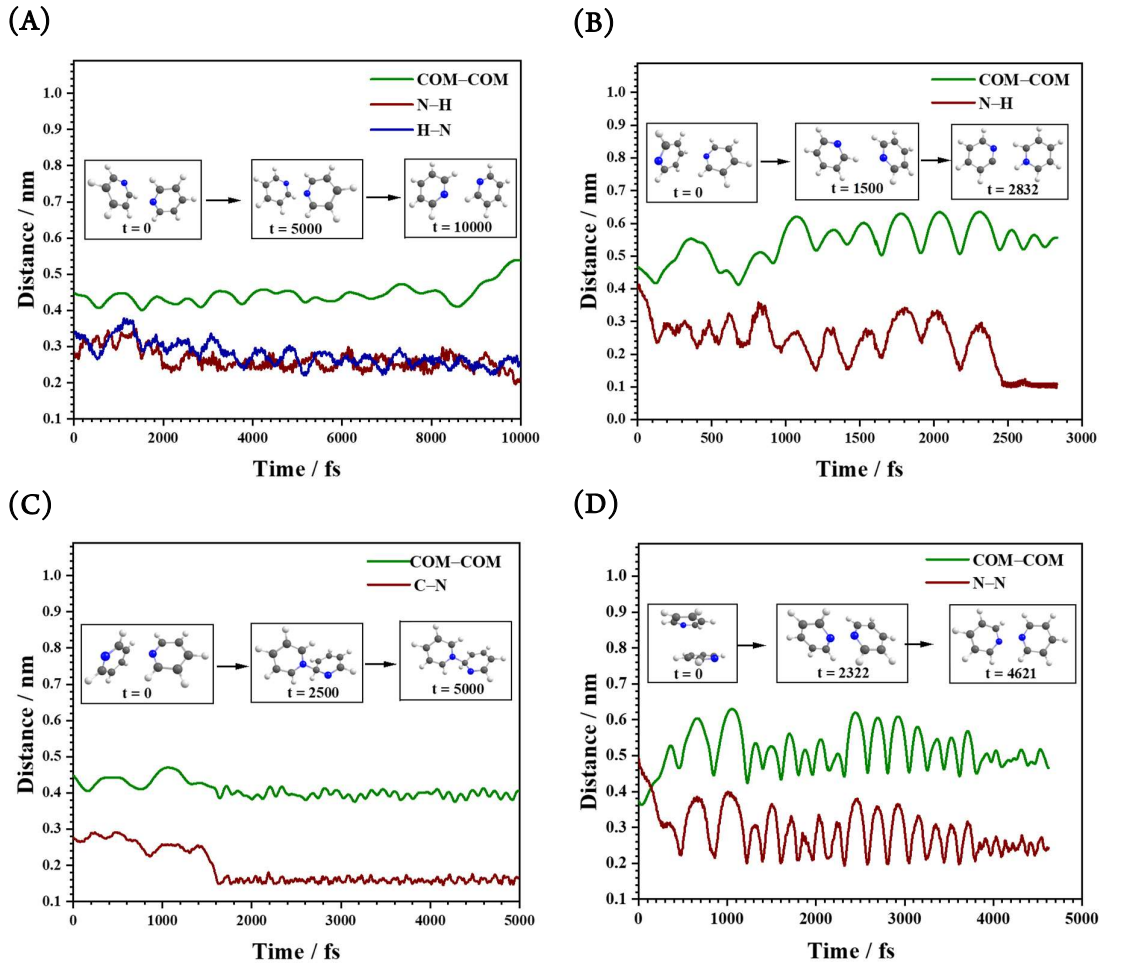

Figure 3. Trajectories showing various reactivity patterns for the pyridine dimer cation. In each plot the COM–COM distance along with an appropriate geometrical parameter is shown. The formation of (A) **[CH···N]** hydrogen-bonded dimer, (B) proton transfer **[PyH–Py]**, (C) **[C–N]** bonded adduct and (D) **[N–N]** bonded adduct is illustrated. The snapshots along the trajectories indicate intermediate structures formed along the roaming pathway to the product formation.

roams over the other and results in the formation of one of the possible four outcomes. Figure 3 illustrates the variation of COM–COM distance and the appropriate geometrical parameter describing the reactivity pattern. The formation of **[CH···N]** hydrogen-bonded dimer is depicted in Figure 3A, while Figure 3B describes the proton transferred structure **[PyH–Py]**, which is a consequence of **[CH···N]** hydrogen bonding. The formation of **[C–N]** and **[N–N]** bonded adducts are also illustrated in formation Figure 3.

The molecular association and the reactivity pattern of the pyridine dimer cation is summarized in Figure 4. The **[CH···N]** hydrogen-bonded dimer is energetically favoured by 0.89 eV (20.5 kcal mol^{-1}), which can also result in the proton transferred structure **[PyH–Py]** with additional stabilization of 0.45 eV (10.4 kcal mol^{-1}). However, only 2/47 trajectories yield proton transferred structure. The formation of **[C –N]** adduct is energetically favourable by 1.70 eV (39.2 kcal mol^{-1}), which gets further stabilized by 0.60 eV (13.8 kcal mol^{-1}) to yield 1,2 proton migrated structure **[1,2–PP]**, which is the most stable form of pyridine dimer cation.[7] However, unlike the structures reported earlier,[7] migration of the proton to the α-position was not observed. Electronic structure calculations

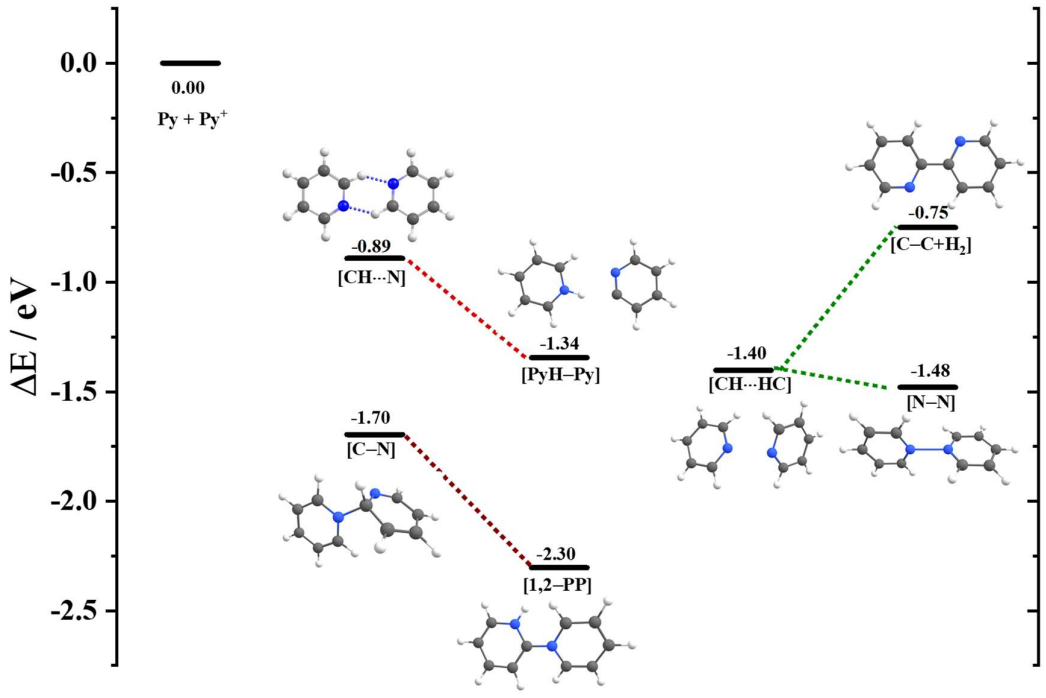

Figure 4. The schematic energy level for various associative/reactive products originating from the pyridine dimer cation calculated at ωb97XD/aug-cc-pVDZ level. The energy scale (eV) is relative to well-separated pyridine dimer cation to pyridine monomer and pyridine radical cation.

carried out at ωb97XD/aug-cc-pVDZ level of theory suggests that even though the migration of the proton to the α-position to yield 1-(2-pyridyl)-pyridin-1-ium cation **[1,2–PP]** is energetically more stable than the **[C–N]** bonded adduct by 0.63 eV (14.5 kcal mol^{-1}), the barrier for the proton migration is about 1.99 eV (45.8 kcal mol^{-1}), which is depicted in Figure S3 (see the SI). Further, as noted earlier, few of the BOMD trajectories also lead to the formation of **[CH···HC]** bonded structures[28–30] (Figure S4, see the SI), competing with the **[N–N]** bonded adduct formation and differ by the dihedral angle between the two pyridine rings, with the **[CH···HC]** bonded structures being planar. However, the **[CH···HC]** bonded structures were found to be metastable and converge to **[N–N]** bonded adduct upon geometry optimization at both BLYP/6-311++G(d,p) and ωb97XD/aug-cc-pVDZ levels of theory. Additionally, loss of dihydrogen (H_2) molecule from the **[CH···HC]** bonded structures to yield bipyridyl radial cation **[C–C]** is unfavourable by 0.65 eV (15.0 kcal mol^{-1}).

IR action spectroscopy of the pyridine dimer cation was used to identify the formation of C–N bonded 1-(2-pyridyl)pyridin-1-ium **[1,2-PP]** structure, which shows a prominent band corresponding to the N–H stretching vibration around 3400 cm^{-1}.[7] The appearance of the N–H stretching vibration can only be attributed to the migration of the proton to the α-position starting from **[C–N]** bonded adduct. Additionally, the IR spectrum also shows a broad and equally strong band in the aromatic C–H stretching region around 3100 cm^{-1}.[7] The calculated IR spectrum of the **[1,2-PP]** structure, depicted in Figure 5, shows much lower (about 20%) intensity in the aromatic C–H stretching region in comparison with the N–H stretching region. It is well-known that the aromatic C–H stretching vibrations are prone to anharmonic coupling,[31–34] however, the total intensity of the transition is derived from the fundamentals. Therefore, the observation of equally intense N–H and aromatic C–H stretching bands suggests that other structural isomers of pyridine dimer cation, such as [**C–N**] bonded adduct, **[N–N]** bonded adduct and proton transferred structure **[PyH–Py]**, all of which show aromatic C–H stretching bands around 3100 cm^{-1}, could possibly contribute to the observed IR spectrum.[7]

CONCLUSION

A comprehensive understanding of the dynamical behaviour of the pyridine dimer cation was accomplished with the aid of Born-Oppenheimer molecular dynamics (BOMD) simulations in

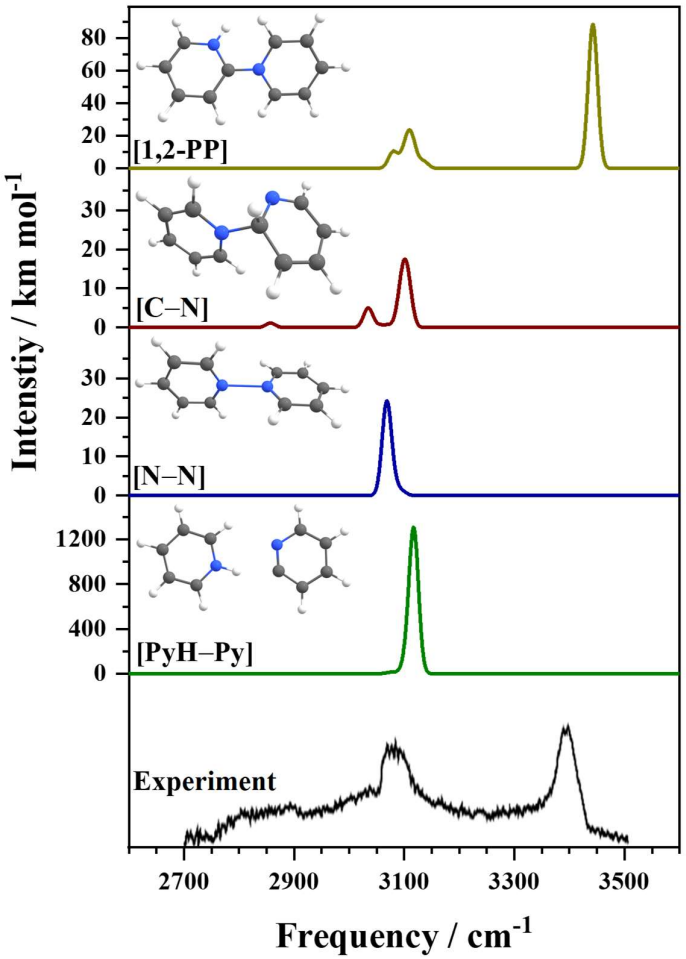

Figure 5. Calculated IR spectra of (top-to-Bottom) α-proton migrated structure **[1,2-PP]**, C–N bond adduct **[C–N]**, N–N bond adduct **[N–N]** and proton transferred structure **[PyH–Py].** The harmonic frequencies were scaled by 0.952 and the IR spectra were broadened with a Gaussian function of 20 cm^{-1} FWHM centered on calculated frequencies. Notice that the y-scale is different for each spectrum. The bottom panel represents the experimental spectrum adopted from Ref. 7.

combination with electronic structure calculations. The BOMD trajectories starting from an anti-parallel π-stacked pyridine dimer in the cationic state, undergo roaming mediated isomerization leading to the molecular association. The C–H···N hydrogen bonded dimer cation was the most prevalent structure, which can undergo occasional proton transfer. Additionally, the formation of C–N and N–N bonded adducts was observed. The C–N bonded adduct does not undergo α-proton migration to yield 1-(2-pyridyl)-pyridin-1-ium cation, as was experimentally observed (Ref. 7), which can be attributed to a rather high barrier for proton migration. Further, metastable C–H···H–C bonded structures were observed in the BOMD simulations, which upon geometry optimization

results in the N–N bonded adduct. The comparison of the experimental (from Ref. 7) and calculated IR spectra indicates that apart from the α-proton migrated structure, other structural isomers such as C–N and N–N bonded adducts are likely to be formed.

Conflicts of interest

There are no conflicts to declare.

ACKNOWLEDGEMENTS

AT thanks IIT Bombay for the Institute Postdoctoral Fellowship. Authors gratefully acknowledge SpaceTime-2 supercomputing facility at IIT Bombay for the computing time. The support and the resources provided by 'PARAM Kamrupa Facility' under the National Supercomputing Mission, Government of India at the Indian Institute of Technology Guwahati are gratefully acknowledged. This study is based upon a work supported in part by the Science and Engineering Research Board of the Department of Science and Technology (Grant no. CRG/2022/005470) and the Board of Research in Nuclear Sciences (BRNS Grant no. 58/14/18/2020) to GNP. Authors wish to thank Mr. Prahlad Roy Chowdhury for his help with electronic structure calculations. Authors also wish to thank the reviewers, whose comments have helped in the considerable improvement of the manuscript.

REFERENCES

(1) Arunan, E.; Gutowsky, H. S. The Rotational Spectrum, Structure and Dynamics of a Benzene Dimer. *J. Chem. Phys.* **1993**, *98*, 4294–4296.

(2) Chandrasekaran, V.; Biennier, L.; Arunan, E.; Talbi, D.; Georges, R. Direct Infrared Absorption Spectroscopy of Benzene Dimer. *J Phys Chem A* **2011**, *115*, 11263–11268.

(3) Erlekam, U.; Frankowski, M.; Meijer, G.; Von Helden, G. An Experimental Value for the B1uC-H Stretch Mode in Benzene. *J. Chem. Phys.* **2006**, *124*, 171101.

(4) Guin, M.; Patwari, G. N.; Karthikeyan, S.; Kim, K. S. A p -Stacked Phenylacetylene and 1 , 3 , 5-Triazine Heterodimer : A Combined Spectroscopic and Ab Initio Investigation. *Phys. Chem. Chem. Phys* **2009**, *11*, 11207–11212.

(5) Guin, M.; Patwari, G. N.; Karthikeyan, S.; Kim, K. S. Do N-Heterocyclic Aromatic Rings Prefer π-Stacking? *Phys. Chem. Chem. Phys.* **2011**, *13*, 5514–5525.

(6) Feng, J. Y.; Lee, Y. P.; Zhu, C. Y.; Hsu, P. J.; Kuo, J. L.; Ebata, T. IR-VUV Spectroscopy of Pyridine Dimers, Trimers and Pyridine-Ammonia Complexes in a Supersonic Jet. *Phys. Chem.*

Chem. Phys. **2020**, *22*, 21520–21534.

(7) Feng, J.; Lee, Y.; Witek, H. A.; Ebata, T. Vacuum Ultraviolet Photoionization Induced Proton Migration and Formation of a New C–N Bond in Pyridine Clusters Revealed by Infrared Spectroscopy and Mass Spectrometry. *J. Phys. Chem. Lett.* **2021**, *12*, 4936–4943.

(8) Hübner, O.; Thusek, J.; Himmel, H.-J. Pyridine Dimers and Their Low-Temperature Isomerization A High-Resolution.Pdf. *Angew. Chem. Int. Ed.* **2023**, *62*, e202218042.

(9) Megiel, E.; Jagielska, A.; Wro, L. A Theoretical and Experimental 14 N NMR Study of Association of Pyridine. *J. Mol. Struct.* **2001**, *569*, 111–119.

(10) Ghosh, S.; Rao Pedireddi, V. Molecular Recognition Studies of Thioamide (–CSNH2) Functionality through Co-Crystals of Some Thiobenzamides with N-Donor Ligands: Evaluation and Correlation of Structural Landscapes with Morphology and Lattice Energy. *Cryst. Growth Des.* **2023**, *23*, 4591–4606.

(11) Meyer, E. A.; Castellano, R. K.; Diederich, F. *Interactions with Aromatic Rings in Chemical and Biological Recognition*; *Angew. Chem. Int. Ed.* **2003**, *42*, 1210–1250.

(12) Mazik, M.; Radunz, W.; Boese, R. Molecular Recognition of Carbohydrates with Acyclic Pyridine-Based Receptors. *J. Org. Chem.* **2004**, *69*, 7448–7462.

(13) Verdejo, B.; Gil-Ramírez, G.; Ballester, P. Molecular Recognition of Pyridine N-Oxides in Water Using Calix[4]Pyrrole Receptors. *J. Am. Chem. Soc.* **2009**, *131*, 3178–3179.

(14) Lavorato, D.; Terlouw, J. K.; Dargel, T. K.; Koch, W.; McGibbon, G. A.; Schwarz, H. Observation of the Hammick Intermediate: Reduction of the Pyridine-2-Ylid Ion in the Gas Phase. *J. Am. Chem. Soc.* **1996**, *118*, 11898–11904.

(15) Samy El-Shall, M.; Ibrahim, Y. M.; Alsharaeh, E. H.; Meot-Ner, M.; Watson, S. P. Reactions between Aromatic Hydrocarbons and Heterocycles: Covalent and Proton-Bound Dimer Cations of Benzene/Pyridine. *J. Am. Chem. Soc.* **2009**, *131*, 10066–10076.

(16) Wu, G.; Stewart, H.; Liu, Z.; Wang, Y.; Stace, A. J. Activation of Methane by the Pyridine Radical Cation and Its Substituted Forms in the Gas Phase. *J. Am. Soc. Mass Spectrom.* **2015**, *26*, 1382–1387.

(17) Golec, B.; Das, P.; Bahou, M.; Lee, Y. P. Infrared Spectra of the 1-Pyridinium (C5H5NH +) Cation and Pyridinyl (C5H5NH and 4-C 5H6N) Radicals Isolated in Solid Para-Hydrogen. *J. Phys. Chem. A* **2013**, *117*, 13680–13690.

(18) Kumar, R.; Li, G.; Gallardo, V. A.; Li, A.; Milton, J.; Nash, J. J.; Kenttämaa, H. I. Measurement of the Proton Affinities of a Series of Mono- And Biradicals of Pyridine. *J. Am. Chem. Soc.* **2020**, *142*, 8679–8687.

(19) Ibrahim, Y.; Mabrouki, R.; Meot-Ner, M.; El-Shall, M. S. Hydrogen Bonding Interactions of Pyridine.+ with Water: Stepwise Solvation of Distonic Cations. *J. Phys. Chem. A* **2007**, *111*, 1006–1014.

(20) Braga, C.; Travis, K. P. A Configurational Temperature Nosé-Hoover Thermostat. *J. Chem. Phys.* **2005**, *123*, 134101.

(21) Vandevondele; Krack, J.; Mohamed, M.; Parrinello, F.; Chassaing, M.;; Hutter, T.; QUICKSTEP: Fast and Accurate Density Functional Calculations Using a Mixed Gaussian and Plane Waves Approach. *Comput. Phys. Commun.* **2005**, *157*, 103–128.

(22) Hutter, J.; Iannuzzi, M.; Schiffmann, F.; Vandevondele, J. Cp2k: Atomistic Simulations of

Condensed Matter Systems. *Wiley Interdiscip. Rev. Comput. Mol. Sci.* **2014**, *4*, 15–25.

(23) VandeVondele, J.; Hutter, J. Gaussian Basis Sets for Accurate Calculations on Molecular Systems in Gas and Condensed Phases. *J. Chem. Phys.* **2007**, *127*, 114105.

(24) Goedecker, S.; Teter, M. Separable Dual-Space Gaussian Pseudopotentials. *Phys. Rev. B - Condens. Matter Mater. Phys.* **1996**, *54*, 1703–1710.

(25) Tagad, A.; Singh, R. K.; Patwari, G. N. Binary Matrix Method to Enumerate, Hierarchically Order, and Structurally Classify Peptide Aggregation. *J. Chem. Inf. Model.* **2022**, *62*, 1585–1594.

(26) Frisch, M. J.; Trucks, G. W.; Schlegel, H. B.; Scuseria, G. E.; Robb, M. A.; Cheeseman, J. R.; Scalmani, G.; Barone, V.; Mennucci, B.; Petersson, G. A.; Nakatsuji, H.; Caricato, M.; Li, X.; Hratchian, H. P.; Izmaylov, A. F.; Bloino, J.; Zheng, G.; Sonnenberg, J. L.; Hada, M.; Ehara, M.; Toyota, K.; Fukuda, R.; Hasegawa, J.; Ishida, M.; Nakajima, T.; Honda, Y.; Kitao, O.; Nakai, H.; Vreven, T.; Montgomery Jr., J. A.; Peralta, J. E.; Ogliaro, F.; Bearpark, M.; Heyd, J. J.; Brothers, E.; Kudin, K. N.; Staroverov, V. N.; Kobayashi, R.; Normand, J.; Raghavachari, K.; Rendell, A.; Burant, J. C.; Iyengar, S. S.; Tomasi, J.; Cossi, M.; Rega, N.; Millam, J. M.; Klene, M.; Knox, J. E.; Cross, J. B.; Bakken, V.; Adamo, C.; Jaramillo, J.; Gomperts, R.; Stratmann, R. E.; Yazyev, O.; Austin, A. J.; Cammi, R.; Pomelli, C.; Ochterski, J. W.; Martin, R. L.; Morokuma, K.; Zakrzewski, V. G.; Voth, G. A.; Salvador, P.; Dannenberg, J. J.; Dapprich, S.; Daniels, A. D.; Farkas, Ö.; Foresman, J. B.; Ortiz, J. V; Cioslowski, J.; Fox, D. J. Gaussian 09, Revision D.01. *Gaussian Inc.* **2009**, Wallingford CT.

(27) Bejoy, N. B.; Singh, R. K.; Singh, N. K.; Pananghat, B.; Patwari, G. N. Dynamics of Hydrogen Bond Breaking Induced by Outer-Valence Intermolecular Coulombic Decay. *J. Phys. Chem. Lett.* **2023**, *14*, 5718–5726.

(28) Wolstenholme, D. J.; Cameron, T. S. Comparative Study of Weak Interactions in Molecular Crystals: H-H Bonds vs Hydrogen Bonds. *J. Phys. Chem. A* **2006**, *110*, 8970–8978.

(29) Singh, P. C.; Patwari, G. N. The C – HÁ Á ÁH – B Dihydrogen Bonded Borane-Trimethylamine Dimer : A Computational Study. *Chem. Phys. Lett.* **2006**, *419*, 265–268.

(30) Singh, P. C.; Patwari, G. N. Theoretical Investigation of C – HÁ Á ÁH – B Dihydrogen Bonded Complexes of Acetylenes with Borane-Trimethylamine. *Chem. Phys. Lett.* **2006**, *419*, 5–9.

(31) Sibert, E. L. Modeling Anharmonic Effects in the Vibrational Spectra of High-Frequency Modes. *Annu. Rev. Phys. Chem.* **2023**, *74*, 219–244.

(32) Singh, S.; Huang, Q. R.; Tan, J. A.; Kuo, J. L.; Patwari, G. N. Ab Initio Anharmonic Analysis of Complex Vibrational Spectra of Phenylacetylene and Fluorophenylacetylenes in the Acetylenic and Aromatic C-H Stretching Region. *J. Chem. Phys.* **2023**, *159*, 104302.

(33) Feng, J. Y.; Huang, Q. R.; Nguyen, H. Q.; Kuo, J. L.; Ebata, T. Infrared–Vacuum Ultraviolet Spectroscopy of the C-H Stretching Vibrations of Jet-Cooled Aromatic Azine Molecules and the Anharmonic Analysis. *J. Chinese Chem. Soc.* **2022**, *69*, 160–172.

(34) Minejima, C.; Ebata, T.; Mikami, N. C-H Stretching Vibrations of Benzene and Toluene in Their S1 States Observed by Double Resonance Vibrational Spectroscopy in Supersonic Jets. *Phys. Chem. Chem. Phys.* **2002**, *4*, 1537–1541.